Journal of Thermal Analysis and Calorimetry
https://doi.org/10.1007/s10973-024-13575-w

Impact of rainfall on smoke dynamics in longitudinally ventilated tunnels: model-scale fire test study

Dia Luan[1,2] · Jakub Bielawski[2,3] · Chuangang Fan[1] · Wojciech Węgrzyńsk[3] · Xinyan Huang[2]

Received: 15 May 2024 / Accepted: 5 August 2024

Abstract
This study investigates the impact of rainfall on smoke dynamics and critical velocity in longitudinally ventilated tunnels through model-scale fire tests. The results show that the maximum ceiling excess temperature decreases as ventilation velocity increases. When rainfall is present, the maximum ceiling excess temperature initially increases and then decreases with higher rainfall intensity. A prediction model has been developed to evaluate the impact of rainfall on the maximum ceiling temperature. The temperature distribution on the side where rainfall occurs is not affected by rainfall itself but is determined solely by ventilation velocity. Additionally, a model has been proposed to predict the decay of the ceiling temperature on the rainfall side. The decay of ceiling temperature on the ventilation side is not influenced by rainfall parameters or fire power when tunnel airflow is primarily driven by either rainfall-induced airflow or ventilation airflow. The presence of rainfall requires a higher critical velocity, and a model for predicting critical velocity has been proposed considering rainfall intensity. This study contributes to our understanding of smoke dynamics in tunnel fires under rainfall conditions and provides valuable insights into smoke control during adverse weather.

Keywords Tunnel fires · Rainfall impact · Smoke dynamics · Critical velocity · Longitudinal ventilation

List of symbols

A_1, a_1, a_2	Fitting parameters in Eq. (5)
A	Pool area (cm^2)
b_f	Equivalent radius of fire source (m)
c_p	Thermal capacity of air (kJ $kg^{-1}K^{-1}$)
d_0	Raindrop size (mm)
g	Gravitational acceleration (m s^{-2})
H	Tunnel height (m)
H_{ef}	Effective tunnel height (m)
ΔHc	Fuel combustion heat (kJ kg^{-1})
I	Rainfall intensity (mm h^{-1})
Kv	Empirical coefficient in Eq. (7)
l_b	Back-layering length (m)
L	Tunnel length (m)
$\dot{m}$	Mass burning rate (kg s^{-1})
Q	Heat release rate (kW)
Q^*	Dimensionless heat release rate (-)
T	Temperature of airflow (K)
ΔT	Gas excess temperature (K)
V	Ventilation velocity (m s^{-1})
V^*	Dimensionless velocity in Eq. (3)
V^{**}	Dimensionless velocity in Eq. (4)
V_{in}	Airflow caused by rainfall (m s^{-1})
V_c^*	Dimensionless critical velocity (-)
x	Distance from reference point (m)

Greek symbols

γ	Scale ratio, equals 15 in our test (-)
ρ	Density (kg m^{-3})
χ	Combustion efficiency (-)

Subscript

a	Ambient condition
max	Maximum value
0	Baseline case, i.e. case without rainfall and ventilation
c	Critical value

✉ Chuangang Fan
chuangang.fan@csu.edu.cn

✉ Xinyan Huang
xy.huang@polyu.edu.hk

1 School of Civil Engineering, Central South University, Changsha, China

2 Department of Building Environment and Energy Engineering, The Hong Kong Polytechnic University, Hong Kong, China

3 Fire Research Department, Building Research Institute, Warsaw, Poland

Published online: 28 September 2024

F	Full scale
M	Model scale

Introduction

Tunnels, as crucial components of transportation infrastructure, play a significant role in enhancing the convenience of people's life. Fire safety in tunnels has always been a major concern due to the catastrophic consequences. For example, the Mont-Blanc tunnel fire in France in 1999 resulted in the tragic death of 31 individuals. Similarly, a truck fire in the Maoliling Tunnel in Zhejiang, China, in 2019 led to five deaths and 31 injuries. Statistics [1, 2] have indicated that smoke is the primary cause of casualties in fire accidents. Due to the limited space and few exits of tunnels, the rapid accumulation of smoke in the event of a fire poses a serious threat to both trapped individuals and the tunnel structure. Therefore, it is vital to promptly implement effective measures to manage and control smoke during a fire.light

Longitudinal ventilation is a widely used smoke control method known for its cost-effectiveness and ease of maintenance. It aims to provide a safe upstream space for evacuation and firefighting by utilizing axial flow fans arranged at the top of the tunnel to generate positive pressure and manage the smoke in the downstream space. Previous scholars have conducted extensive research on smoke dynamics in longitudinally ventilated tunnels.

The ceiling temperature is widely concerned as a key parameter for evaluating fire risk and determining the performance of fire protection systems. Kurioka et al. [3] conducted a series of reduced-scale experiments and developed an empirical prediction expression for the maximum ceiling temperature in a longitudinally ventilated tunnel, but the model is not applicable to tunnel fires under low ventilation velocity. Hu et al. [4] studied smoke temperature distribution along the tunnel ceiling through large-scale and full-scale tunnels tests. Results indicate that the dimensionless excess temperature distributions along tunnel ceiling followed a consistent exponential decay pattern across all tests, despite variations in fire size, height above the floor, tunnel geometry, and ventilation velocity. Li et al. [5] conducted a series of model-scale tunnel fire tests, fully considering the low ventilation, and proposed a prediction model for the maximum ceiling excess gas temperature, which is divided into two regions based on the dimensionless ventilation velocity. Ji et al. [6] investigated the influence of transverse fire locations on the maximum ceiling temperature through model-scale tunnel fire tests. Results showed that the restrictive effect of the tunnel sidewalls caused an increase in the maximum ceiling temperature for fires near the sidewall in comparison to fires located at the longitudinal centerline of the tunnel. Ingason et al. [7] carried out a series of tunnel fire tests to investigate critical parameters for HGV (Heavy Goods Vehicle) fire, including the maximum ceiling temperature and temperature distribution. Results showed that for large-scale HGV fires with HRR (heat release rate) greater than 100 MW, HRR and ventilation have less impact on the maximum smoke temperature. Additionally, the dimensionless ceiling excess temperature decreases exponentially with the dimensionless distance from the fire source. Gong et al. [8] theoretically analyzed the heat and mass transfer during the smoke movement, considering the heat convection with tunnel roof, as well as heat loss due to the air entrainment and heat radiation. They proposed a model with a double exponential term for predicting the temperature distribution, which was validated by model-scale tests. Zhao et al. [9] conducted a series of fire experiments to investigate the temperature distribution in a longitudinally ventilated metro tunnel and found that the upstream temperature distribution was more sensitive to the ventilation than downstream.

A key parameter of managing smoke such fires in longitudinally ventilated tunnels is the concept of "critical velocity". If the ventilation velocity is low, fire smoke can flow upstream, against the direction of the ventilation airflow. This reverse flow is called "back-layering". The "critical velocity" is the ventilation velocity that can just eliminate back-layering, which is the lowest required ventilation to maintain a clear upstream space. Thomas [10] was among the first to focus on the critical velocity, believing that smoke spread would stop when the buoyancy of the fire smoke equals the inertial force of the ventilation airflow. However, he only considered small fire cases with flames significantly smaller than the tunnel height. Oka and Atkinson [11] and Li et al. [12] fully considered the fire size and carried out a series of small-scale tunnel tests to explore the correlation between the critical velocity and HRR. Although there were differences in HRR values for critical velocity transition, these two studies upheld a consistent segmentation rule based on HRR values. This rule states that the dimensionless critical velocity is proportional to the 1/3 power of dimensionless HRR in small fires, while it remains independent of HRR in large fires. However, the analysis conducted by these researchers did not take into account the tunnel width. Wu and Baker [13] investigated the effect of tunnel geometry on critical ventilation and suggested that hydraulic diameter is a more appropriate characteristic length than tunnel height in dimensionless analysis. This viewpoint has also been supported by Kang [14]. Tsai et al. [15] investigated the influence of fire location from the tunnel exit, and the results showed that the critical velocity decreases as the fire approaches the tunnel exit. Additionally, the influence of other factors, such as tunnel slope [16–18], blockage [19–21], fire source amount [22–24], and tunnel structure [25–27], on critical ventilation velocity has also been widely investigated.

To sum up, the field of smoke dynamics and critical velocity in longitudinally ventilated tunnels is relatively well-established, primarily influenced by tunnel geometry, fire scale, and boundary conditions. However, our recent studies [28, 29] have shown that ambient rainfall can induce longitudinal airflow in tunnels by causing local pressure changes. When longitudinal ventilation opposes the rain-induced airflow, the interaction between the two airflows can complicate the dynamics of fire smoke. Additionally, it is reasonable to assume that higher critical velocities are required to mitigate the impact of rain-induced airflow compared to conditions without rainfall.

The primary objective of this study is to examine the impact of rainfall on smoke dynamics and critical velocity in longitudinally ventilated tunnels, considering the increasing frequency of heavy rainfall events. This research is valuable for enhancing emergency response capabilities in tunnel engineering under extreme conditions, ultimately leading to improved safety and readiness in challenging environmental situations.

Experimental

Reduced-scale experiments play a crucial role in fire research due to their advantages, such as good repeatability, low cost, and ease of control, compared to full-scale tunnel fire tests. In reduced-scale fire research, it is essential to carefully choose a scaling criterion to ensure that the findings from small-scale tests can be extrapolated to real fire situations [30]. The Froude criterion is suitable for studying the flow for fire smoke related to buoyancy. Our findings [28, 29] indicate that rainfall affects fire behavior by creating an airflow inside the tunnel, allowing fire smoke to be mainly driven by buoyancy and forced force. Thus, the scaling laws of Froude criterion can be applied to fire research under rainfall conditions. However, it should be noted that experimental results may vary slightly from the actual scenario as not all parameters may adhere to the scaling criterion simultaneously, especially regarding heat transfer [31, 32]. The movement and temperature field of fire smoke have already been proved to show a good scaling relationship to the full size in previous studies [7, 33], which is the focus of our research. Table 1 lists the key parameters of the Froude criterion.

Fire tests were conducted on a reduced-scale experimental platform ($\gamma = 15$) consisting of a model tunnel, an artificial rainfall simulator, and an axial flow fan. Dimensions of the model tunnel are 10 m in length, 0.6 m in width, and 0.4 m in height. The artificial rainfall simulator, located on one side of the tunnel, allows for the adjustment of rainfall intensity and raindrop size. More details about the artificial rainfall simulator can be found in previous work [28, 29]. The other side of the tunnel is connected to an axial fan, the airflow is equalized by a rectifier, and the ventilation velocity is adjusted by a frequency converter. The schematic of the experimental platform is shown in Fig. 1. Generally, in ventilation tunnels, the tunnel side with ventilation is called upstream, while the other side is called downstream.

Table 1 Scaling correlations of the Froude criterion

Parameters	Symbol	Scaling correlations
Length	L /m	$L_F = \gamma L_M$
Heat release rate	Q /kW	$Q_F = \gamma^{5/2} Q_M$
Rainfall intensity	I /mm h-1	$I_F = \gamma^{1/2} I_M$
Raindrop size	d_0 /mm	$d_{0F} = \gamma^{1/2} d_{0M}$
Mass flow rate	$\dot{m}$/kg s^{-1}	$\dot{m}_F = \gamma^{5/2} \dot{m}_M$
Velocity	V /m s-1	$V_F = \gamma^{1/2} V_M$
Temperature	T /K	$T_F = T_M$

A square pool with a depth of 4 cm was placed at the center of the tunnel, with absolute ethanol chosen as the fuel. The initial fuel depth was set at 1 cm to allow for sufficient time for quasi-steady combustion, enabling a comparative analysis of the impact of wind and rainfall. The fuel's mass loss was monitored using an electronic balance with a precision of 0.1 g, and the HRR can be obtained by the real time burning rate, using the formula below:

$$Q = \chi \dot{m} \Delta Hc \tag{1}$$

where, $\dot{m}$ is the fuel's burning rate, while χ and ΔHc represent the combustion efficiency and fuel combustion heat, respectively. For liquid ethanol, these values are 0.994 and 26,800 kJ kg^{-1}, respectively. A total of 51 K-type thermocouples with a diameter of 1 mm were arranged 0.02 m below the tunnel ceiling to measure the ceiling temperature and back-layering length. Two pool area sizes, six rainfall intensities, two raindrop sizes, and six ventilation velocities were examined in this study. A total of 132 cases were carried out, with each test repeated at least twice to ensure the reliability of the results. The details of the tests conducted are shown in Table 2. Figure 2 shows the burning rate under varying rainfall and ventilation conditions, with error bars included. The small errors indicate the high repeatability of the tests.

Results and discussion

Maximum gas temperature beneath the ceiling

Figure 3a shows the change in maximum ceiling excess temperature under varying rainfall and ventilation conditions. Airflow tilts the fire flame and subsequently affects

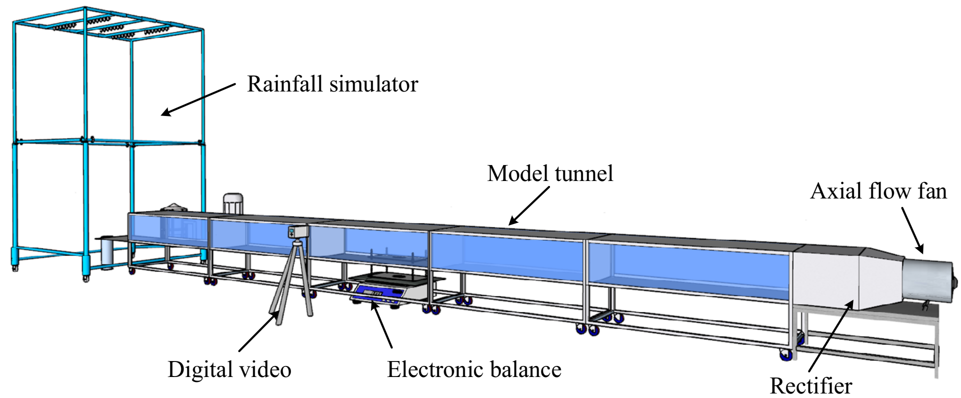

Fig. 1 Schematic of the experimental platform

Table 2 Summary of conducted tests, where the values in [] are equivalent in full-scale condition

Case No	Rainfall intensity I/mm h^{-1}	Raindrop size d_0/mm	Pool area A/cm^2	HRR Q/kW	Ventilation velocity V/m s^{-1}
1–12	0 [0]	1.0 [4]	64	2.1 [1800]	0 [0]
13–36	20 [77]	1.5 [6]	144	6.7 [5900]	0.26 [1.0]
37–60	30 [116]				0.39 [1.5]
61–84	40 [155]				0.52 [2.0]
85–108	50 [194]				0.65 [2.5]
109–132	60 [232]				0.78 [3.0]

HRR shown is a baseline value without rainfall and ventilation

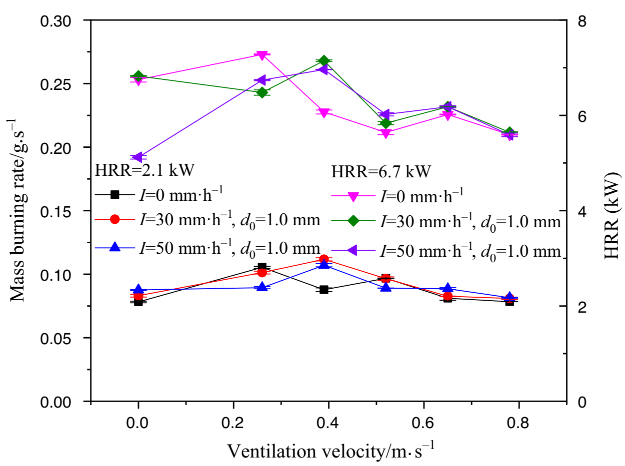

Fig. 2 Burning rate under varying rainfall and ventilation conditions

the burning rate, leading to the changes in maximum ceiling excess temperature. Generally, ventilation airflow tilts the flame in the absence of rainfall, resulting in reduced heat radiation from the flame reaching the ceiling, and consequently lowering the maximum ceiling temperature. In cases, where the fire is influenced by two opposite airflows from rainfall and ventilation, the flame tends to lean in the downstream direction of the dominant airflow, referring to Fig. 3b, taking the cases of HRR = 6.7 kW, $I = 30$ and 50 mm h^{-1} as examples. Rainfall occurs on the left side of the tunnel, while ventilation airflow enters from the right end of the tunnel. As a result, the flame inclination gradually shifts from right to left with increasing ventilation at a constant rainfall intensity. When the two airflows are evenly balanced, the flame remains upright. Usually, a smaller flame tilt angle from the vertical direction indicates higher radiation heat feedback from the flame to the ceiling and consequently higher maximum ceiling excess temperatures.

Li et al. [5] proposed a prediction model for the maximum gas excess temperature beneath the ceiling in a longitudinal ventilation tunnel fire, as follows:

$$\Delta T_{\max} = \begin{cases} 17.5\dfrac{Q^{2/3}}{H_{\mathrm{ef}}^{5/3}}, & V^* \le 0.19 \\ \dfrac{Q}{V b_{\mathrm{f}}^{1/3} H_{\mathrm{ef}}^{5/3}}, & V^* > 0.19 \end{cases} \tag{2}$$

where

$$V^* = V \Big/ \left(\frac{gQ}{b_{\mathrm{f}} c_{\mathrm{p}} \rho_{\mathrm{a}} T_{\mathrm{a}}}\right)^{1/3} \tag{3}$$

The maximum ceiling excess temperature obtained from the experiment shows good agreement with Li's model [5] when there is no rainfall and only ventilation is applied, as shown in Fig. 4a.

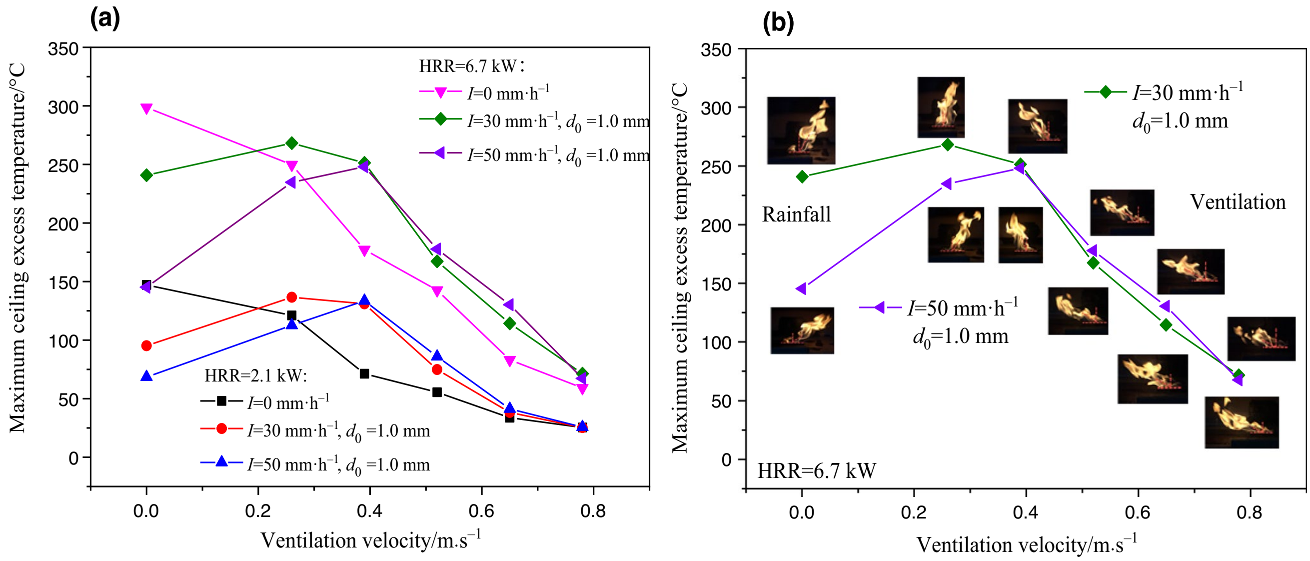

Fig. 3 **a** Changes in maximum ceiling excess temperature under varying rainfall and ventilation conditions, **b** Fire flames for cases of HRR = 6.7 kW, I = 30 and 50 mm h^{-1} vary with ventilation

When there is rainfall on one side of the tunnel, the ceiling maximum temperature increases first and then decreases as ventilation velocity increases. Previous work [28, 29] indicates the velocity of airflow caused by rainfall (denoted by V_{in}) increases with the rainfall intensity, while decreasing with raindrop size, and it follows the correction of $V_{in} \propto I^{1/2}d_0^{-1/4}$. Using cases without rainfall and ventilation as the baseline, the term of $\Delta T_{max}/\Delta T_{max,0}$ is used to characterize the change in maximum temperature caused by rainfall and ventilation. The term of Q/Q_0 is used to characterize the change in heat release rate caused by rainfall and ventilation. The dimensionless velocity is defined as $V^{**} = \frac{I^{1/2}d_0^{-1/4}g^{1/4}b_f^{1/2}}{V}$ to characterize the dominant airflow. The relationship between the dimensionless excess temperature, dimensionless heat release rate, and dimensionless velocity is shown in Fig. 4b. Thus, a prediction model for the maximum ceiling excess temperature is established considering the combined effects of rainfall and ventilation, as follows:

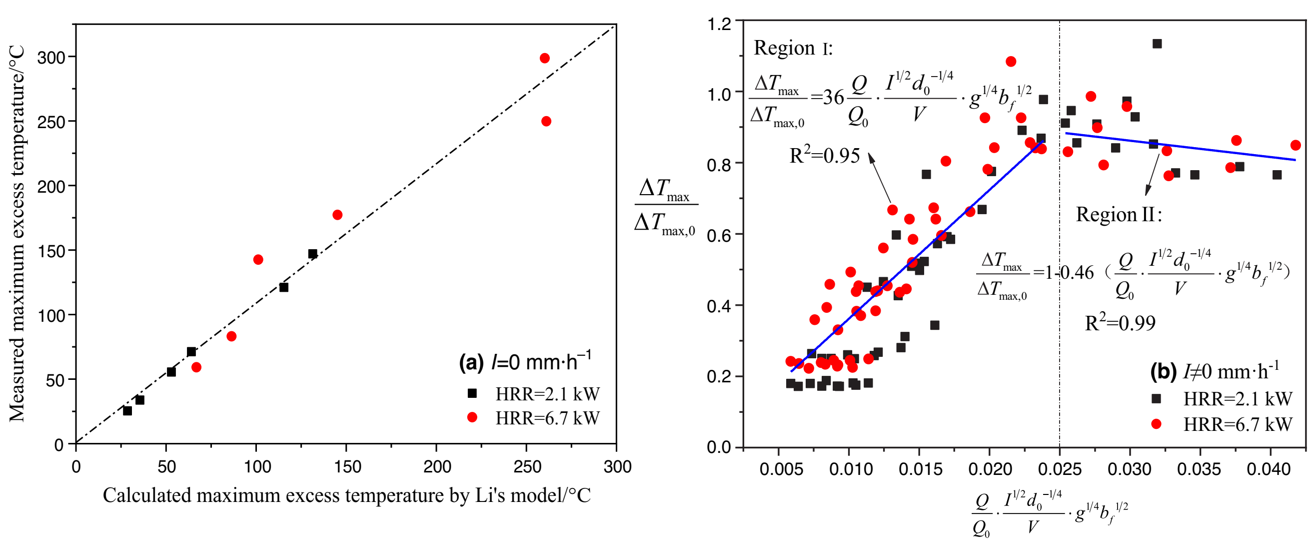

Fig. 4 **a** Comparison of experimental and Li's model [5] for maximum ceiling excess temperature when I = 0 mm h^{-1}; **b** Relationship between the dimensionless excess temperature, dimensionless heat release rate, and dimensionless velocity when $I \neq 0$ mm h.$^{-1}$

$$\frac{\Delta T_{max}}{\Delta T_{max,0}} = \begin{cases} 36\frac{Q}{Q_0} \cdot \frac{I^{1/2} d_0^{-1/4} g^{1/4} b_f^{1/2}}{V}, \frac{I^{1/2} d_0^{-1/4} g^{1/4} b_f^{1/2}}{V} & \leq 0.025 \\ 1 - 0.46\left(\frac{Q}{Q_0} \cdot \frac{I^{1/2} d_0^{-1/4} g^{1/4} b_f^{1/2}}{V}\right), \frac{I^{1/2} d_0^{-1/4} g^{1/4} b_f^{1/2}}{V} & > 0.025 \end{cases}, I \neq 0\,\mathrm{mm\,h^{-1}} \tag{4}$$

Ceiling gas temperature distribution

The fire plume rises driven by buoyancy and then spreads one-dimensionally along the tunnel ceiling, constrained by the side walls. As the smoke progresses along the tunnel ceiling, heat loss occurs due to air entrainment and heat transfer, leading to a decrease in ceiling temperature. Previous studies [8, 9, 34] have confirmed the exponential decay of the ceiling temperature with spreading distance, and some prediction model have been developed. Gong's model [8], which incorporates a double exponential term, has become the most commonly used empirical equation, as follows:

$$\frac{\Delta T}{\Delta T_{max}} = A_1 \cdot \exp\left[-a_1\left(\frac{x_{max} - x}{H}\right)\right] + \left(1 - A_1\right) \cdot \exp\left[-a_2\left(\frac{x_{max} - x}{H}\right)\right] \tag{5}$$

where, A_1, a_1 and a_2 are just fitting parameters.

Taking the cases of HRR = 6.7 kW as examples, Fig. 5 shows the distribution of ceiling excess temperature under various rainfall and ventilation conditions. The horizontal coordinate represents the distance from the fire source, with positive values indicating the ventilation side and negative values indicating the rainfall side. In the absence of rainfall, smoke movement on the ventilation side is hindered, and the smoke is managed in the downstream space once the ventilation velocity reaches the critical velocity. As ventilation velocity increases, the maximum ceiling temperature decreases, and its location tends to move further away from the fire source. When both rainfall and ventilation are present, the smoke experiences conflicting airflows, causing it to spread further on the ventilation side compared to conditions without rainfall. In cases, where rainfall-induced airflow dominates, the maximum ceiling temperature is located upstream of the fire source and gradually shifts downstream with increasing ventilation velocity. Moreover, under the same rainfall intensity and ventilation velocity, smoke disperses over a shorter distance on the ventilation side for a larger raindrop size.

In a tunnel fire scenario, smoke initially moves forward along the tunnel ceiling due to thermal buoyancy until it reaches a point, where the resistance, primarily from wall friction, balances the buoyancy force. This specific point, where the smoke stops is known as the "smoke stagnation point". The airflow caused by rainfall increases the resistance for smoke movement towards the tunnel portal with rainfall, leading to a shorter diffusion length from the fire source compared to conditions without rainfall. Three types of smoke movement can occur depending on the competition between rainfall-induced airflow and longitudinal ventilation airflow, as shown in Fig. 6. If ventilation airflow dominates over rainfall-induced airflow, the smoke stagnation point appears on the ventilation side (see Fig. 6a). Conversely, if rainfall-induced airflow is stronger than ventilation airflow, the smoke stagnation point appears on the rainfall side (see Fig. 6b). When the two airflows are balanced, the smoke moves toward both ends of the tunnel influenced by both airflows (see Fig. 6c).

Cold air is continuously entrained during the movement of hot smoke, and heat exchange occurs between the hot smoke and the tunnel wall and surrounding space. These leads to a gradual decrease in smoke temperature as it spreads. A dimensionless method is employed to analyze the relationship between ceiling excess temperature and spreading distance, with the point of maximum ceiling excess temperature serving as a reference. Figure 7 shows the decay of the dimensionless ceiling excess temperature on the rainfall side with the dimensionless distance from the reference point for cases with HRR = 6.7 kW. It is observed that the temperature decay on the rainfall side is sensitive to both rainfall intensity and raindrop size when there is no ventilation, i.e., $V = 0$ m s^{-1}, which has been reported in previous work [28, 29]. However, once longitudinal ventilation is activated, the temperature decay on the rainfall side is determined solely by ventilation velocity and is no longer affected by rainfall.

Equation 5 is utilized to analyze the variation of ceiling temperature decay on the rainfall side when $V > 0$ m s^{-1}, and the relationship between decay coefficients and ventilation velocity is shown in Fig. 8. It is evident that the ceiling temperature decay coefficients on the rainfall side are less affected by fire power. As a result, Eq. 6 can well predict the ceiling temperature decay on the rainfall side under the combined effects of rainfall and ventilation, as follows:

$$\frac{\Delta T}{\Delta T_{max}} = (0.14V + 0.52) \cdot \exp\left[(2.56V - 2.56)\frac{x_{max} - x}{H}\right] + (-0.14V + 0.48) \cdot \exp\left[(0.21V - 0.17)\frac{x_{max} - x}{H}\right] \tag{6}$$

here, $V > 0$ m s^{-1}.

Similarly, the decay of the ceiling temperature on the ventilation side is also analyzed, as shown in Fig. 9. It is observed that when the ventilation velocity is significantly lower than (see Fig. 9a and b) or much higher than (see Fig. 9d) the rainfall-induced airflow, meaning the dominant airflow in the tunnel from one of them, the decay of the ceiling temperature on the ventilation side remains unaffected by rainfall parameters and fire power. However, when the ventilation velocity falls within the range of induced airflow

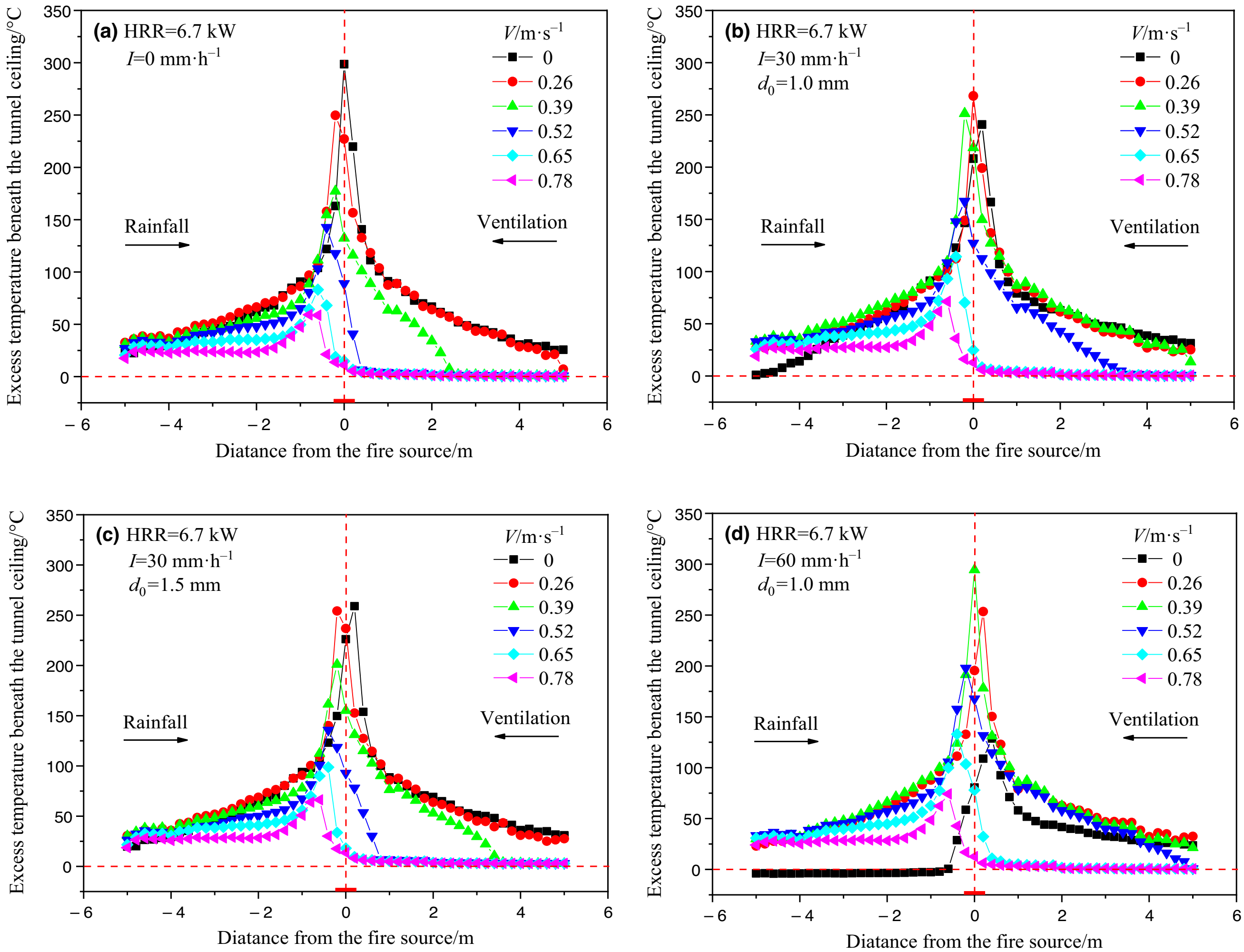

Fig. 5 Distribution of ceiling excess temperature under various rainfall and ventilation conditions

Fig. 6 Three types of smoke movement under effects of rainfall-induced and ventilation airflows

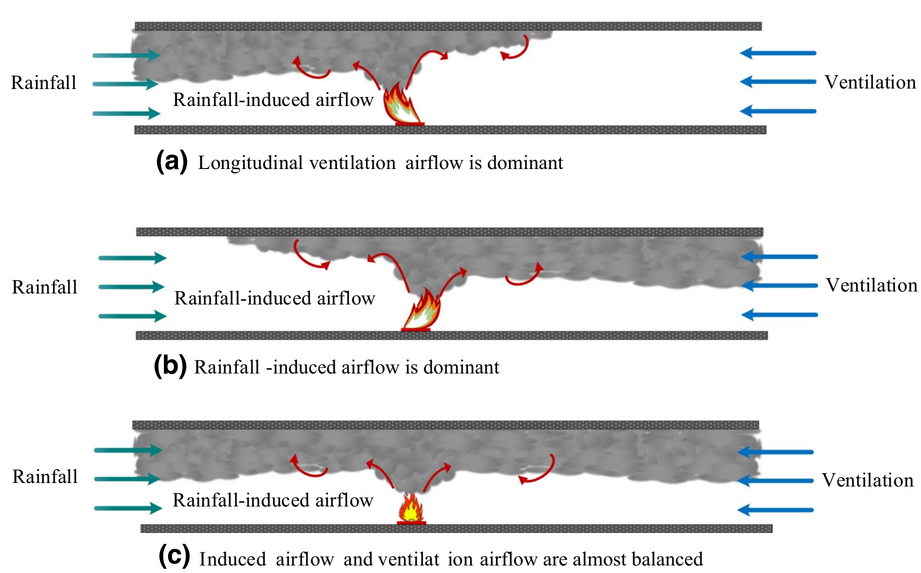

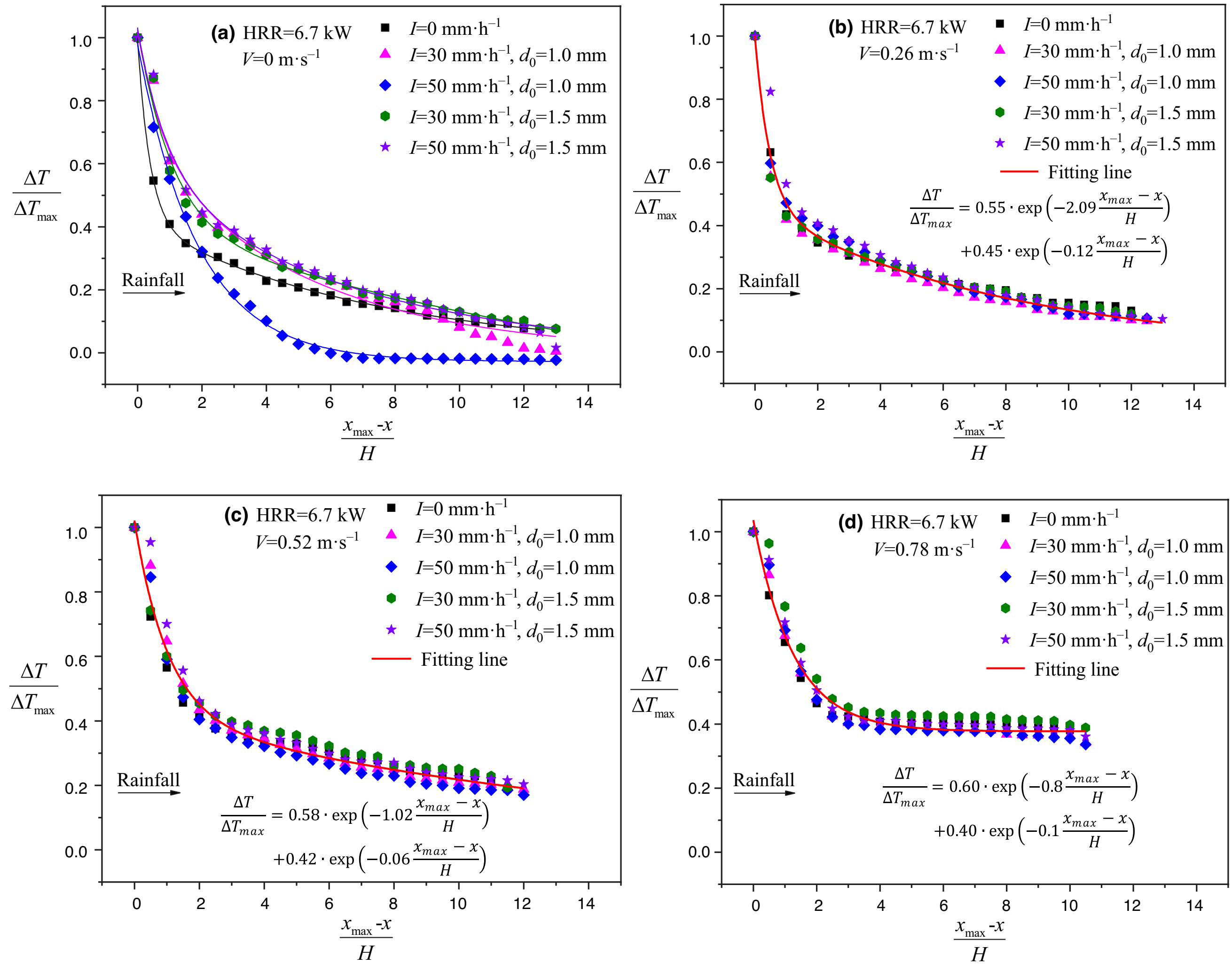

Fig. 7 Decay of the ceiling excess temperature on the rainfall side with spreading distance

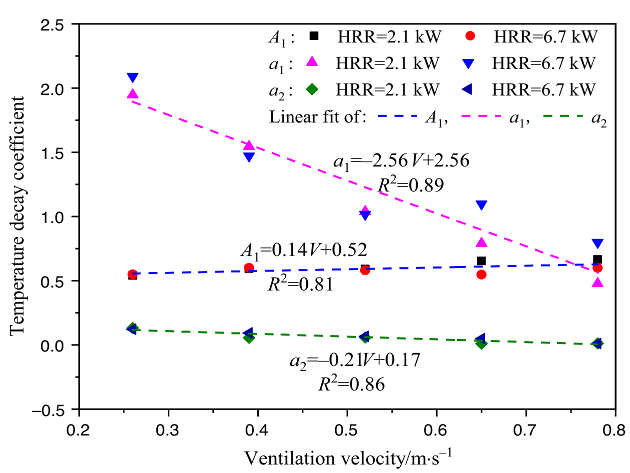

Fig. 8 Temperature decay coefficients of rainfall side with ventilation velocity ($V>0$ m s.$^{-1}$)

[28, 29] (see Fig. 9c), the smoke flow condition transitions from Fig. 6a, b as rainfall intensity increases, and the temperature attenuation on the ventilation side is notably influenced by rainfall.

Back-layering length and critical ventilation

The back-layering length and critical velocity are crucial parameters for tunnel fire safety and ventilation system design. The distance from the fire source to the smoke stagnation point is known as the back-layering length, denoted as l_b. The position of the smoke stagnation point is determined by a significant decrease in ceiling temperature. When thermocouple A records a much higher temperature than adjacent thermocouple B, and thermocouple B is close to ambient temperature, the smoke stagnation point is determined to be at the location of thermocouple A [21, 35]. An example is provided to clarify the smoke stagnation point and the

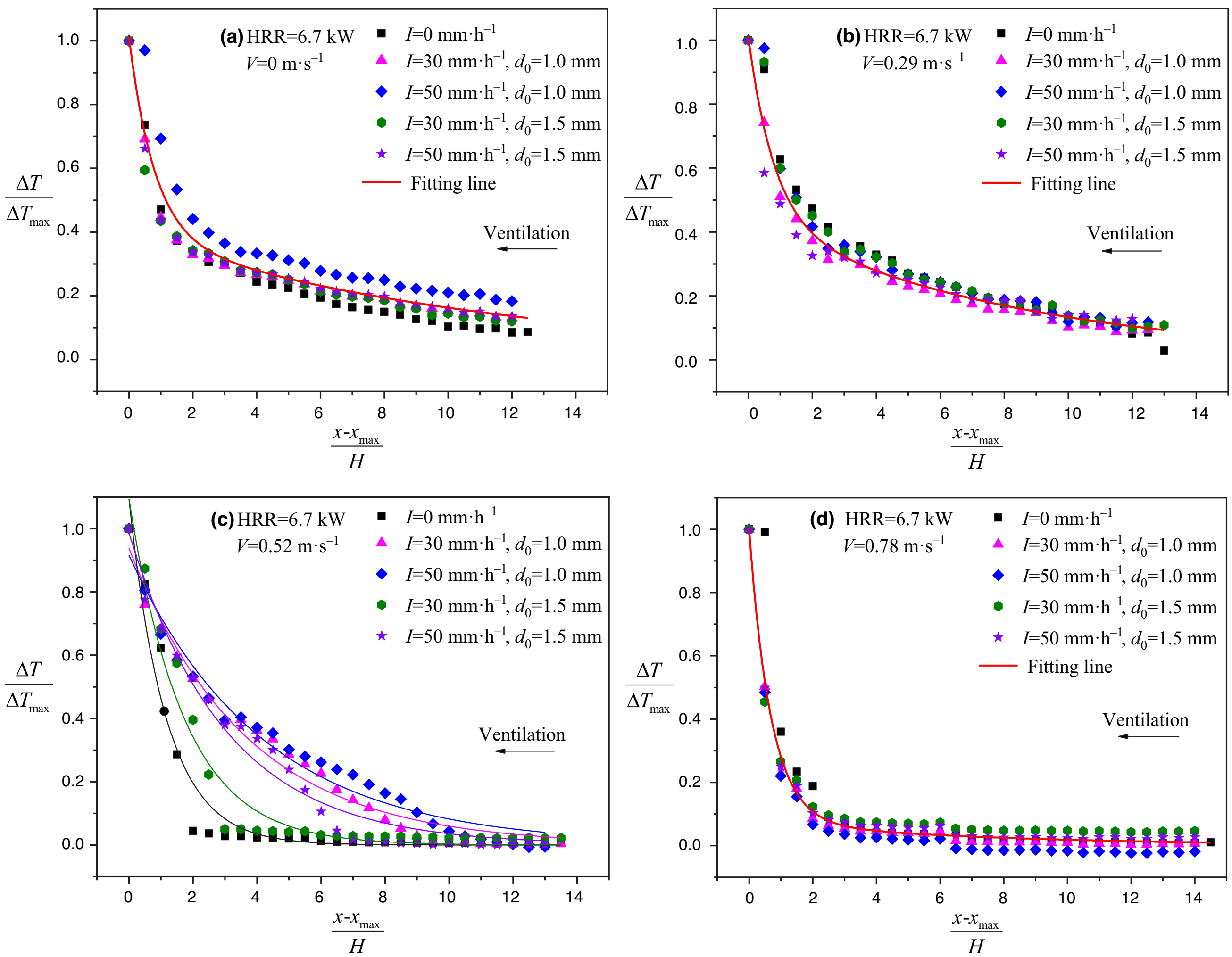

Fig. 9 Decay of the ceiling excess temperature on the ventilation side with spreading distance

back-layering length. Figure 10 provides the typical ceiling temperature distribution with varying ventilation velocities. According to the judgment method mentioned, the smoke back-layering length is 3.8 m at a ventilation velocity of 0.26 m s^{-1}, and it reduces to 0.6 m at a ventilation velocity of 0.39 m s^{-1}. In cases, where the sudden temperature drop occurs downstream of the fire source, the back-layering length is denoted by a negative value. For instance, the back-layering length is −0.6 m at a ventilation velocity of 0.78 m s^{-1}, indicating a higher ventilation velocity than the critical velocity. It can be speculated that the critical velocity, at which the smoke back-layering length becomes 0, lies between 0.39 m s^{-1} and 0.78 m s^{-1}.

Figure 11 shows the change in back-layering length under varying rainfall and ventilation conditions, using cases with HRR = 2.1 kW as examples. The back-layering length varies linearly with ventilation velocity, except in cases, where smoke overflows from the tunnel. The interpolation method [36] is used to determine the critical velocity. Table 3 lists the

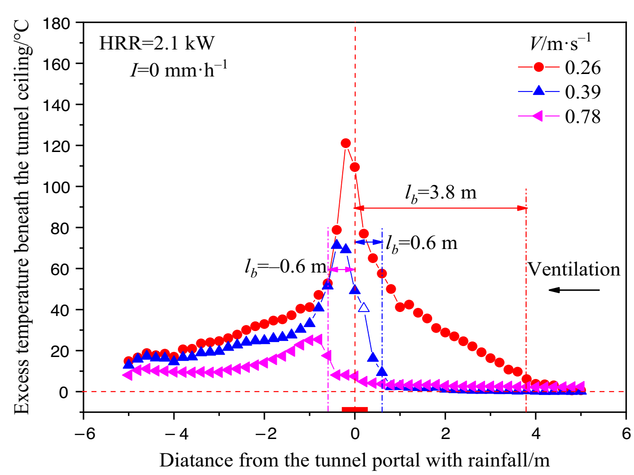

Fig. 10 Typical ceiling temperature distribution with varying ventilation velocities

critical velocity information for two fire sizes under different rainfall conditions. It can be found that the back-layering length decreases as ventilation velocity increases under the same rainfall condition. When ventilation velocity remains constant, the back-layering length tends to increase with higher rainfall intensity. Moreover, for the same rainfall intensity and ventilation velocity, a larger raindrop size results in a shorter back-layering length.

Prediction models for the critical velocity proposed by Oka and Atkinson [11] and Li et al. [12] are as follows:

Oka and Atkinson's model [11]:

$$V_c^* = \begin{cases} Kv\left(\frac{Q^*}{0.12}\right)^{1/3}, & Q^* < 0.12 \\ Kv, & Q^* \geq 0.12 \end{cases} \tag{7}$$

where

$$V_c^* = V_c \Big/ \sqrt{gH} \tag{8}$$

$$Q^* = Q/\rho_0 c_p T_0 g^{1/2} H_{ef}^{5/2} \tag{9}$$

Here, Kv is an empirical coefficient in the range of 0.22–0.38.

Li's model [12]:

$$V_c^* = \begin{cases} 0.81Q^{*1/3}, & Q^* \leq 0.15 \\ 0.43, & Q^* > 0.15 \end{cases} \tag{10}$$

Although the empirical formulas for critical velocity from them differ, the basic understanding is consistent. Specifically, the dimensionless critical velocity V_c^* increases with the 1/3 power of the dimensionless heat release rate Q^* for small fires, and V_c^* becomes independent of Q^* for large fires. The fire sizes considered in this study are relatively small ($Q^* < 0.12$), thus the dimensionless critical velocity is only related to the dimensionless heat release rate. When rainfall works, the critical ventilation velocity is not only related to the dimensionless heat release rate but also to rainfall parameters. Using cases without rainfall as the baseline, the term of $V_c^* \Big/ V_{c,0}^*$ is used to characterize the change in critical velocity caused by rainfall, then we can obtain the correction of $\frac{V_c^*}{V_{c,0}^*} \sim \left[\frac{Q^*}{Q_0^*}, I, d_0\right]$, $I > 0$ mm h^{-1}. The critical velocity required increases due to the presence of rainfall. Figure 12 shows the relationship of $V_c^* \Big/ V_{c,0}^*$ as a function of

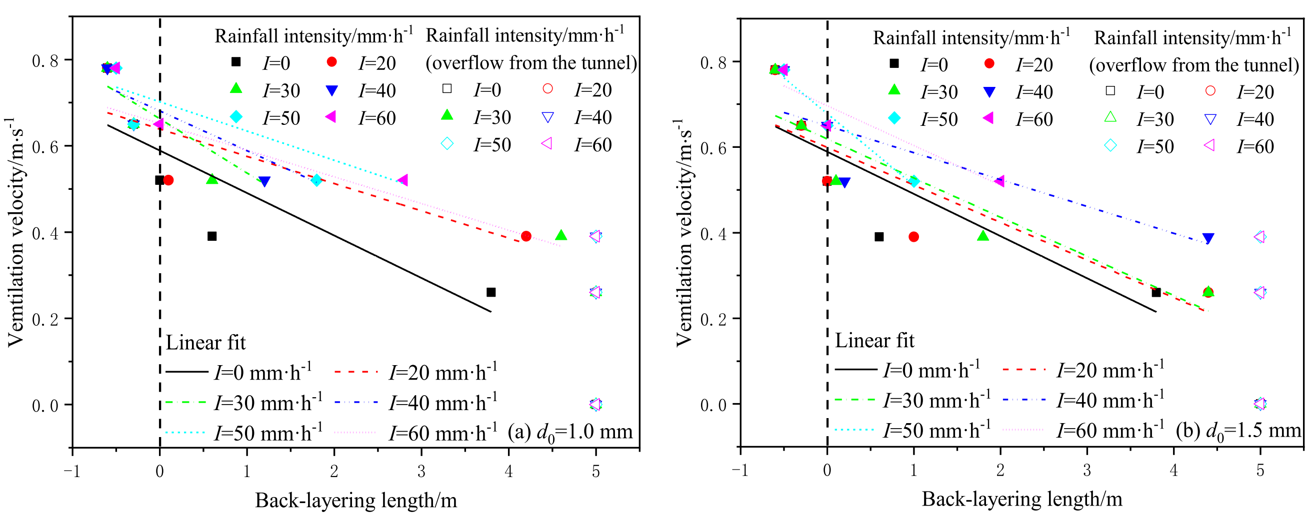

Fig. 11 Changes in back-layering length vary rainfall and ventilation conditions (HRR = 2.1 kW)

Table 3 Critical velocity for two fire sizes under different rainfall conditions [unit: m s^{-1}]

HRR	V_c										
	I mm/h^{-1}										
	0	20		30		40		50		60	
	d_0/mm										
	–	1.0	1.5	1.0	1.5	1.0	1.5	1.0	1.5	1.0	1.5
2.1 kW	0.589	0.638	0.599	0.652	0.619	0.662	0.649	0.681	0.678	0.702	0.696
6.7 kW	0.639	0.689	0.673	0.711	0.684	0.715	0.687	0.722	0.719	0.732	0.729

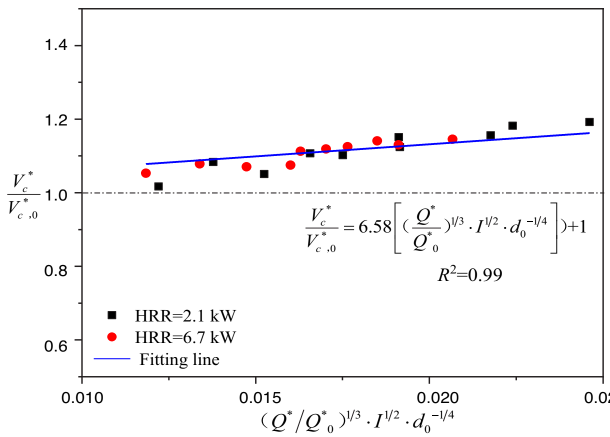

Fig. 12 Increased critical velocity caused by rainfall

$\left[\left(\frac{Q^*}{Q_0^*}\right)^{1/3}\cdot I^{1/2}\cdot d_0^{-1/4}\right]$ for cases with $I > 0$ mm h^{-1}. When $I = 0$ mm h^{-1}, the term of $V_c^* / V_{c,0}^*$ should be 1. Thus, $\frac{V_c^*}{V_{c,0}^*} = 6.58\left[\left(\frac{Q^*}{Q_0^*}\right)^{1/3}\cdot I^{1/2}\cdot d_0^{-1/4}\right] + 1$. As a result, the critical velocity of the tunnel fire under the effect of rainfall can be predicted by Eq. 11.

$$\frac{V_c^*}{V_{c,0}^*} = 6.58\left[\left(\frac{Q^*}{Q_0^*}\right)^{1/3}\cdot I^{1/2}\cdot d_0^{-1/4}\right] + 1 \tag{11}$$

Conclusions

This work conducts a series of reduced-scale tunnel fire tests to study the impact of rainfall on smoke dynamics and critical velocity in a longitudinally ventilated tunnel. The following are the main conclusions:

(1) Under the influence of two opposing airflows from rainfall-induced and ventilation, the fire flame tends to tilt downstream direction of the dominant airflow. When rainfall is present, the maximum ceiling excess temperature initially increases and then decreases with higher rainfall intensity. A prediction model for the maximum ceiling excess temperature is established considering the combined effects of rainfall and ventilation.

(2) The decay of the ceiling temperature on the rainfall side is influenced only by ventilation velocity once ventilation is activated. The decay of the ceiling temperature on the ventilation side remains unaffected by rainfall parameters and fire power, as long as the ventilation velocity is significantly lower or much higher than the rainfall-induced airflow. A prediction model for the ceiling temperature decay on the rainfall side is developed.

(3) The back-layering length decreases as ventilation velocity increases but increases with higher rainfall intensity. Higher critical velocity is required due to the presence of rainfall. A model has been proposed to evaluate the increases in critical velocity caused by rainfall. It is noted that the HRR ranges from 2.1 to 6.7 kW in this work, equivalent to 2 to 6 MW in full-scale. The applicability of a wider HRR needs to be verified.

Acknowledgements This work is supported by National Natural Science Foundation of China (Grant No. 52278545), the Key Research and Development Program of Hunan Province (Grant No. 2022SK2093), the Natural Science Foundation of Hunan Province of China (Grant No. 2024JJ2075), and Hong Kong Research Grants Council Theme-based Research Scheme (T22-505/19-N). Additionally, we are grateful for resources from the High Performance Computing Center of Central South University.

Authors contribution Dia Luan involved in methodology, investigation, data curation, writing—original draft; Jakub Bielawski involved in review and editing the paper; Chuangang Fan involved in conceptualization, resources, supervision, funding acquisition; Wojciech Węgrzyński involved in review and editing the paper; Xinyan Huang involved in writing—review and editing, Supervision, Funding acquisition.

Funding Open access funding provided by The Hong Kong Polytechnic University.

Declarations

Competing interest The authors declare that they have no known competing financial interests or personal relationships that could have appeared to influence the work reported in this paper.

References

1. Babrauskas V, Gann RG, Levin BC, Paabo M, Harris RH, Peacock RD, et al. A methodology for obtaining and using toxic potency data for fire hazard analysis. Fire Saf J. 1998;31:345–58. https://doi.org/10.1016/S0379-7112(98)00013-7.
2. Leistikow B, Martin D, Milano C. Fire injuries, disasters, and costs from cigarettes and cigarette lights: a global overview. Prev Med. 2000;31:91–9. https://doi.org/10.1006/pmed.2000.0680.

3. Kurioka H, Oka Y, Satoh H, Sugawa O. Fire properties in near field of square fire source with longitudinal ventilation in tunnels. Fire Saf J. 2003;38:319–40. https://doi.org/10.1016/S0379-7112(02)00089-9.
4. Hu L, Huo R, Wang H, Li Y, Britter R. Experimental studies on fire-induced buoyant smoke temperature distribution along tunnel ceiling. Build Environ. 2007;42:3905–15. https://doi.org/10.1016/j.buildenv.2006.10.052.
5. Li Y, Lei B, Ingason H. The maximum temperature of buoyancy-driven smoke flow beneath the ceiling in tunnel fires. Fire Saf J. 2011;46:204–10. https://doi.org/10.1016/j.firesaf.2011.02.002.
6. Ji J, Fan C, Zhong W, Shen X, Sun J. Experimental investigation on influence of different transverse fire locations on maximum smoke temperature under the tunnel ceiling. Int J Heat Mass Transf. 2012;55:4817–26. https://doi.org/10.1016/j.ijheatmasstransfer.2012.04.052.
7. Ingason H, Li YZ. Model scale tunnel fire tests with longitudinal ventilation. Fire Saf J. 2010;45:371–84. https://doi.org/10.1016/j.firesaf.2010.07.004.
8. Gong L, Jiang L, Li S, Shen N, Zhang Y, Sun J. Theoretical and experimental study on longitudinal smoke temperature distribution in tunnel fires. Int J Therm Sci. 2016;102:319–28. https://doi.org/10.1016/j.ijthermalsci.2015.12.006.
9. Zhao S, Liu F, Wang F, Weng M. Experimental studies on fire-induced temperature distribution below ceiling in a longitudinal ventilated metro tunnel. Tunn Undergr Space Technol. 2018;72:281–93. https://doi.org/10.1016/j.tust.2017.11.032.
10. P Thomas. The movement of smoke in horizontal passages against an air flow. Fire Res Stn Note No 723 Fire Res Stn UK Sept. 1968.
11. Oka Y, Atkinson G. Control of smoke flow in tunnel fires. Fire Saf J. 1995;25:305–22. https://doi.org/10.1016/0379-7112(96)00007-0.
12. Li Y, Lei B, Ingason H. Study of critical velocity and backlayering length in longitudinally ventilated tunnel fires. Fire Saf J. 2010;45:361–70. https://doi.org/10.1016/j.firesaf.2010.07.003.
13. Wu Y, Bakar M. Control of smoke flow in tunnel fires using longitudinal ventilation systems—a study of the critical velocity. Fire Saf J. 2000;35:363–90.
14. Kang K. Characteristic length scale of critical ventilation velocity in tunnel smoke control. Tunn Undergr Space Technol. 2010;25:205–11. https://doi.org/10.1016/j.tust.2009.11.004.
15. Tsai K, Lee Y, Lee S. Critical ventilation velocity for tunnel fires occurring near tunnel exits. Fire Saf J. 2011;46:556–7. https://doi.org/10.1016/j.firesaf.2011.08.003.
16. Yi L, Xu Q, Xu Z, Wu D. An experimental study on critical velocity in sloping tunnel with longitudinal ventilation under fire. Tunn Undergr Space Technol. 2014;43:198–203. https://doi.org/10.1016/j.tust.2014.05.017.
17. Chow W, Gao Y, Zhao J, Dang J, Chow C, Miao L. Smoke movement in tilted tunnel fires with longitudinal ventilation. Fire Saf J. 2015;75:14–22. https://doi.org/10.1016/j.firesaf.2015.04.001.
18. Du T, Yang D, Ding Y. Driving force for preventing smoke backlayering in downhill tunnel fires using forced longitudinal ventilation. Tunn Undergr Space Technol. 2018;79:76–82. https://doi.org/10.1016/j.tust.2018.05.005.
19. Lee Y, Tsai K. Effect of vehicular blockage on critical ventilation velocity and tunnel fire behavior in longitudinally ventilated tunnels. Fire Saf J. 2012;53:35–42. https://doi.org/10.1016/j.firesaf.2012.06.013.
20. Gannouni S, Maad R. Numerical study of the effect of blockage on critical velocity and backlayering length in longitudinally ventilated tunnel fires. Tunn Undergr Space Technol. 2015;48:147–55. https://doi.org/10.1016/j.tust.2015.03.003.
21. Meng N, Hu X, Tian M. Effect of blockage on critical ventilation velocity in longitudinally ventilated tunnel fires. Tunn Undergr Space Technol. 2020;106: 103580. https://doi.org/10.1016/j.tust.2020.103580.
22. Tsai K, Chen H, Lee S. Critical ventilation velocity for multi-source tunnel fires. J Wind Eng Ind Aerodyn. 2010;98:650–60. https://doi.org/10.1016/j.jweia.2010.06.006.
23. Tang F, Deng L, Meng N, Mcnamee M, Van Hees P, Hu L. Critical longitudinal ventilation velocity for smoke control in a tunnel induced by two nearby fires of various distances: experiments and a revisited model. Tunn Undergr Space Technol. 2020;105: 103559. https://doi.org/10.1016/j.tust.2020.103559.
24. Meng N. Experimental study on flame merging behaviors and smoke backlayering length of two fires in a longitudinally ventilated tunnel. Tunn Undergr Space Technol. 2023;137: 105147. https://doi.org/10.1016/j.tust.2023.105147.
25. Liu C, Zhong M, Song S, Xia F, Tian X, Yang Y, et al. Experimental and numerical study on critical ventilation velocity for confining fire smoke in metro connected tunnel. Tunn Undergr Space Technol. 2020;97: 103296. https://doi.org/10.1016/j.tust.2020.103296.
26. Huang Y, Li Y, Li J, Wu K, Li H, Zhu K, et al. Experimental investigation of the thermal back-layering length in a branched tunnel fire under longitudinal ventilation. Int J Therm Sci. 2022;173: 107415. https://doi.org/10.1016/j.ijthermalsci.2021.107415.
27. Chen C, Jiao W, Zhang Y, Shi C, Lei P, Fan C. Experimental investigation on the influence of longitudinal fire location on critical velocity in a T-shaped tunnel fire. Tunn Undergr Space Technol. 2023;134: 104983. https://doi.org/10.1016/j.tust.2023.104983.
28. Fan C, Luan D, Bu R, Sheng Z, Wang F, Huang X. Can heavy rainfall affect the burning and smoke spreading characteristics of fire in tunnels? Int J Heat Mass Transf. 2023;207: 123972. https://doi.org/10.1016/j.ijheatmasstransfer.2023.123972.
29. Luan D, Bu R, Sheng Z, Fan C, Huang X. Experimental study on the impact of asymmetric heavy rainfall on the smoke spread and stratification dynamics in tunnel fires. Tunn Undergr Space Technol. 2023;134: 104992. https://doi.org/10.1016/j.tust.2023.104992.
30. Ingason H, Li YZ, Lönnermark A. (2015) Tunnel Fire Dynamics. New York, NY: Springer New York. https://doi.org/10.1007/978-1-4939-2199-7
31. Hurley MJ, Gottuk D, Hall JR, Harada K, Kuligowski E, Puchovsky M, et al., (2016) editors. SFPE Handbook of Fire Protection Engineering. New York, NY: Springer New York. https://doi.org/10.1007/978-1-4939-2565-0
32. Ingason H, Li YZ, Lönnermark A. (2024) Tunnel Fire Dynamics. Cham: Springer International Publishing. https://doi.org/10.1007/978-3-031-53923-7
33. Li J, Liu W, Li YF, Chow WK, Chow CL, Cheng CH. Scale modelling experiments on the effect of longitudinal ventilation on fire spread and fire properties in tunnel. Tunn Undergr Space Technol. 2022;130: 104725. https://doi.org/10.1016/j.tust.2022.104725.
34. Kashef A, Yuan Z, Lei B. Ceiling temperature distribution and smoke diffusion in tunnel fires with natural ventilation. Fire Saf J. 2013;62:249–55. https://doi.org/10.1016/j.firesaf.2013.09.019.
35. Guo F, Gao Z, Wan H, Ji J, Yu L, Ding L. Influence of ambient pressure on critical ventilation velocity and backlayering distance of thermal driven smoke in tunnels with longitudinal ventilation. Int J Therm Sci. 2019;145: 105989. https://doi.org/10.1016/j.ijthermalsci.2019.105989.
36. Gwon H, Seung R, Hong S. An experimental study on the effect of slope on the critical velocity in tunnel fires. J Fire Sci. 2010;28:27–47. https://doi.org/10.1177/0734904109106547.